MATERIAL CHARACTERIZATION FOR COMPRESSION RESIN TRANSFER MOLDING PROCESS SIMULATION

M. Vollmer[1], N. Tagscherer[1], S. Zaremba[1], D. Schultheiß[2], P. Mertiny[3] and K. Drechsler[1]

[1]Chair of Carbon Composites, TUM Department of Mechanical Engineering,
Technical University of Munich, Boltzmannstr. 15, 85748 Garching, Germany
Email: vollmer@lcc.mw.tum.de, Web Page: http://www.lcc.mw.tum.de
[2]KDX Europe Composites R&D Center GmbH, Am Weiglfeld 15, 83629 Weyarn, Germany
[3]Advanced Composite Materials Engineering Group, Department of Mechanical Engineering,
University of Alberta, 9211-116 Street NW, Edmonton, Alberta, Canada

Keywords: Compression Resin Transfer Molding, CRTM, simulation, simulation input, material characterization, viscosity, permeability, compaction, compression, epoxy, NCF

Abstract
Compression resin transfer molding (CRTM) has been shown to be a promising manufacturing process for automotive applications. CRTM optimization via simulation has been subject of various studies, yet these studies do not adequately assess the material characterization used to get their simulation input. The present paper aims to close this gap by presenting methods for characterizing the resin and reinforcement phase, then discussing test results for two typical automotive materials. An epoxy resin system was characterized by viscosity measurements using a rotational rheometer. The viscosity was observed to remain at a low level for a certain transition time, followed by an exponential rise. This transition time decreased with increasing temperature. In-plane and out-of-plane permeability tests with the chosen biaxial carbon fiber non-crimp fabric (NCF) were performed for fiber volume fraction (FVF) ranging from 40% to 60%, showing a strong dependency between FVF and permeability. The compaction behavior of the NCF was characterized for two compaction rates. Observed differences in the stress-strain curves indicate viscoelastic compaction behavior. The present study demonstrates that the utilized test methodologies are suitable to characterize the input parameters needed for CRTM simulation. Using the presented material database as simulation input provides a starting point for future CRTM software verification and process optimization.

1. Introduction

Short cycle time and low cost are the main requirements for carbon fiber reinforced plastic (CFRP) manufacturing in the automotive industry. Until now these requirements have been met by optimizing CFRP manufacturing processes, among other factors, for serial production: in particular compression molding and high-pressure resin transfer molding (RTM) [1]. However, previous studies show that another RTM variant, i.e. compression resin transfer molding (CRTM), is also capable of meeting automotive requirements [2,3].

The CRTM process, as schematically illustrated in Figure 1, can be described by its two main process phases: the resin injection and the compaction phase. During the first phase, an upper rigid mold section is partially closed, enabling either a gap between the preform and mold or a not fully compacted preform. This facilitates the injection of resin with minimum flow-resistance into the gap or the more permeable preform. After a defined amount of resin has been injected, the CRTM compaction phase starts by fully closing the mold. During the mold closure, the preform is being fully impregnated with resin and compacted to the final part thickness [4].

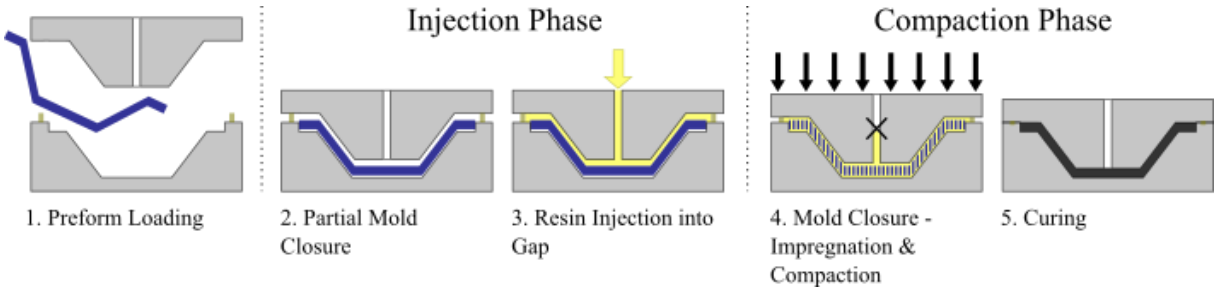

Figure 1: Schematic illustration of CRTM process steps, grouped into resin injection and compaction phase.

One option for an effective realization of CRTM relies on simulation software to advance and optimize this process. Various academic studies have investigated different aspects of the CRTM process [5–8], yet none of these studies fully describe the material characterization that is needed for the simulation input. The present paper attempts to fill this gap by discussing experimental procedures to generate the needed input for CRTM simulation, as well as presenting results of a comprehensive material characterization.

2. Required Input Data for CRTM Simulation

The resin flow in CFRP manufacturing has generally been modeled obeying Darcy's law (Eq. 1), which describes fluid flow through a porous medium. The flow of the fluid is hereby described by its velocity vector $\vec{v}$, the permeability tensor $\boldsymbol{K}$ of the porous medium, the driving pressure gradient ∇P, and the viscosity μ of the fluid. While pressure is a process variable, viscosity and permeability are characteristics of the constituent materials and need to be thoroughly characterized prior to any simulation [9].

$$\vec{v} = -\frac{\boldsymbol{K}}{\mu} * \nabla P \tag{1}$$

Resin systems used in CFRP manufacturing commonly exhibit a non-Newtonian behavior. A higher process temperature generally lowers resin viscosity. Simultaneously, the resin curing increases viscosity over time. As per Darcy's law (Eq. 1), a low resin viscosity at elevated temperature is desired to minimize preform filling times. However, good knowledge of the temperature specific cure kinetics is essential to prevent a premature viscosity increase, risking uncomplete preform filling [9]. Therefore, a thorough characterization of the resin viscous behavior over time at process temperatures is essential to generate required input data for CRTM simulation [10].

Applying Darcy's law (Eq. 1) in composite manufacturing simulation, a good understanding of the permeability of the reinforcement is required. During some CFRP manufacturing processes, i.e. RTM, the preform impregnation of thin structures is dominated by in-plane resin flow at a constant mold thickness. Therefore, the permeability characterization for these processes can be narrowed down to in-plane permeability tests at one desired fiber volume fraction (FVF). Conversely, the preform impregnation at CRTM takes place during its injection and during its compaction phase. At the latter, the preform is compressed whereby its permeability is continuously changed. Additionally, a significant part of the preform impregnation during the compaction phase occurs by in-plane and through-thickness resin flow [4,11]. These process specifics require an extensive reinforcement characterization, specifically, its in-plane and out-of-plane permeability over a wide range of FVFs, as input for CRTM simulation [4,10].

In addition to the resin viscosity and reinforcement permeability, the compaction behavior of the reinforcement is needed to adequately model the CRTM process. During the CRTM compaction phase, the loading acting on the mold σ_{mold} is, according to the one-dimensional laminate consolidation approach (Eq. 2) of Gutowski et al. [12], balanced by the resin pressure P and the stress needed to compact the preform σ_{pref}.

$$\sigma_{mold} = P + \sigma_{pref} \tag{2}$$

To accurately predict mold forces and model the resin flow resulting from the continuous change in permeability, the reinforcement's resistance to compaction σ_{pref} has to be determined as input for CRTM simulation [10,11]. The three input variables, resin viscosity, reinforcement permeability and compaction behavior, are characterized in detail throughout the following sections.

3. Viscosity of Resin

Viscosity is defined as the resistance of a fluid against deformation or flow [9]. Therefore, a good knowledge about the resin's viscosity behavior is needed to accurately model the resin flow during the CRTM process. According to Advani and Sozer [9], the viscosity of most thermoset resins is a function of pressure, temperature, degree of cure and shear rate. In the following, a thermoset resin system is characterized by its isothermal viscosity development over time at constant shear rate.

3.1. Experimental Procedure – Viscosity

Viscosity measurements were performed on the Modular Compact Rheometer (MCR) 302 (Anton Paar, Graz, Austria). Isothermal rotatory measurements were performed at three process-relevant temperature levels: 80°C, 100°C and 120°C. A cone-plate measurement set up was used with radius R_{CP} = 12.5 mm and cone angle of α_{CP} = 1° according to DIN 53019. A gap of 50 µm beneath the cone was calibrated for each temperature level. Based on preliminary tests the shear rate for all measurements was set to $\dot{\gamma} = 100\ s^{-1}$. Tests for each temperature level were repeated in triplicate for statistical relevance.

3.2. Material and Sample Preparation – Viscosity

A warm curing epoxy resin system from Huntsman (The Woodlands, Texas, United States) was chosen for the present study, typical for automotive applications [13]. The epoxy resin, Araldite® LY 3585, and the amine hardener, Aradur® 3475, were processed as per the manufacturer's data sheet [14]. The individual components were degassed, weighed and manually stirred at room temperature for approximately 45 seconds. The time measurement for the viscosity tests was initiated as soon as the evenly mixed resin system was dispensed onto the heated sample carrier of the rheometer. At the same time, the automatic closing of the rheometer was started, leading to a temporal offset between the start of the experiment and the first recorded data point.

3.3. Results – Viscosity

The diagram on the left-hand side of Figure 2 displays the measured viscosity versus time for the investigated epoxy system up to η = 700 mPa.s. The three displayed viscosity curves exhibit common characteristics in term of initial viscosity at a low level followed by an exponential rise in viscosity. Having the shear rate fixed for all measurements, the results show a clear temperature dependency of the viscosity, indicated by an earlier viscosity rise for tests at higher temperature. The diagram on the right-hand side of Figure 2 depicts data points up to η = 50 mPa.s. Even though the first 30 to 40

seconds of the measurements could not be recorded, the level of the initial viscosity at the first recorded data points is shown to be below 10 mPa.s for all three temperature levels.

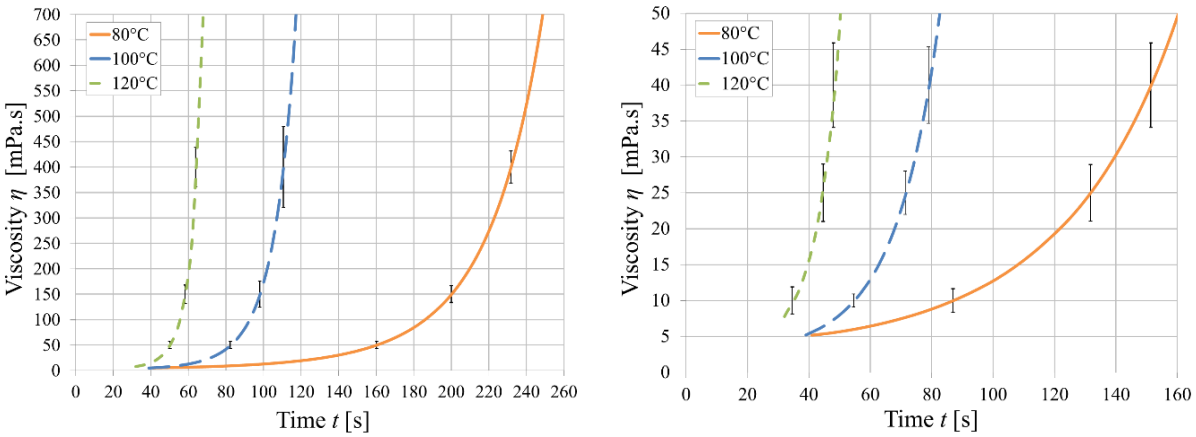

Figure 2: Isothermal viscosity measurements over time of three temperatures – epoxy resin system: Araldite® LY 3585 and Aradur® 3475 (mean of tests performed in triplicate; standard deviation shown as error bar).

3.4. Discussion – Viscosity

The presented results indicate a strong temperature dependency of the viscosity behavior. A higher temperature generally promotes curing of the resin system leading to fast cross-linking of the prepolymer [9]. Exact knowledge of the curing kinetics is crucial to optimize CRTM processes towards short cycle times by enabling resin infusion at low viscosity, as well as initiating an early cure as soon as the preform is fully impregnated.

Overall, the reproducibility of the performed measurements was good, ensured by strict and consistent measurement procedure, performed by the same operator. However, significant differences were identified comparing the measured viscosity values to the data provided by the manufacturer [14]. For the latter, the viscosity rises approximately 30% earlier in time for all measured temperature levels. These discrepancies can be explained by different mixing procedures, a different definition of the measurement start, and different test method or testing parameters, i.e. shear rate [15].

4. Permeability of Reinforcement

Generally, the permeability of a porous material is defined as the inverse of the quantity describing the medium's resistance to fluid flow. The general second order permeability tensor K can be diagonalized, consisting of two principal in-plane permeabilities K_1 and K_2 and of one principal out-of-plane (or through-thickness) permeability K_3. The principal in-plane permeabilities can be graphically described by an ellipsis, commonly defining K_1 as of largest magnitude and rotated by the angle β relative to the coordinate system of the reinforcement [9].

Besides its anisotropic nature, the permeability of reinforcement fabrics depends mainly on its textile type and on its FVF, thus the compaction of the reinforcement [9,16]. In the following, the permeability tensor of a carbon fiber non-crimp fabric (NCF) is characterized for a FVF range of 40% to 60% to determine input data for CRTM simulation.

4.1. Experimental Procedure – Permeability

To this day, no specific method has been standardized to measure the permeability of reinforcement fabrics, therefore, a wide variety of experimental procedures exist [17–19]. For the present study, the permeability test facilities at the Chair of Carbon Composites, Technical University of Munich, were used [20].

Saturated, out-of-plane permeability measurements were carried out using the (one-dimensional) '1D Out-of-Plane Facility' explained by Meier et al. [20]. A 3 mm spacer was used for all tests, resulting in a consistent preform thickness of 3 mm during testing. The fluid flow was evenly distributed over the 124 mm preform diameter by 340-hole perforated plates, each hole measuring a diameter of 4 mm.

Unsaturated, in-plane permeability measurements were performed via the (two-dimensional) '2D In-Plane Facility' as explained in [20]. In accordance to the out-of-plane permeability tests, all preforms were compressed to a thickness of 3 mm prior to in-plane measurements. The preform height during the experiments was controlled by the displacement control of the universal testing machine (UTM) Inspekt table 100 (Hegewald & Peschke, Nossen, Germany). In addition, more accurate measurements from two laser distance sensors were used during data postprocessing. The development of the radial-flow-front was optically recorded and analyzed using MATLAB (MathWorks, Natrick, Massachusetts, United States) in order to calculate K_1 and K_2 as well as their rotational angle β. All in-plane and out-of-plane permeability tests were performed in triplicate to ensure statistical relevance.

4.2 Materials and Sample Preparation – Permeability

A stitched, biaxial, carbon fiber NCF was chosen for the present study, manufactured by SGL Group (Wiesbaden, Germany) and denoted SIGRATEX® C B310/45-ST-E214/5g [21]. The fabric has a specific weight of 310 g/m^2 and 5 g powder binder, Araldite® LY 3366 (Huntsman), is sintered to its upper side.

As explained in the previous section, all preforms were tested at a height of 3 mm, for which the different FVFs for different test set ups were adjusted by the number of reinforcement layers. Preforms consisting of 7, 8, 9 and 10 layers were carefully cut and stacked, intending to measure permeabilities at fiber volume fractions V_f = 41.7%, 47.7%, 53.8% and 59.6%, respectively. Preforms of 0.3 m squares were binder-activated at 170°C ± 10°C via infrared heating and debulked under vacuum pressure prior to permeability testing, to be compliant to industrial manufacturing processes. Preliminary tests showed that preforms of less than 8 layers remained after debulking at heights lower than the desired testing thickness of 3 mm; therefore these preforms should have been excluded. To be able to measure at least one FVF lower than 47.7% (8 layers), it was decided to activate preforms of 7 layers only under heat without compaction, yielding adequate preform heights for testing.

Non-reactive sunflower oil was used as test fluid for all permeability measurements. Its Newtonian behavior was verified and its viscosity was measured at 52.9 mPa.s, at 25.5°C, on the Modular Compact Rheometer (MCR) 302 of Anton Paar.

4.3. Results – Permeability

The results of the radial, in-plane permeability measurements are shown in the diagram on the left-hand side of Figure 3. Values of K_1 and K_2 as well as for their rotational angle β are listed in Table 1. Both principal in-plane permeabilities decreased with increasing fiber volume fraction, showing a similar non-linear trend for K_1 as for K_2. The measured permeabilities drop by nearly one order of magnitude between 40.7% to 56.4% fiber volume fraction, with decreasing standard deviations.

The results of the out-of-plane permeability measurements are presented on the graph on the right-hand side of Figure 3. K_3 shows a trend of reduced permeability at increased fiber volume fraction, again exhibiting a permeability drop of one order of magnitude over the tested FVF range.

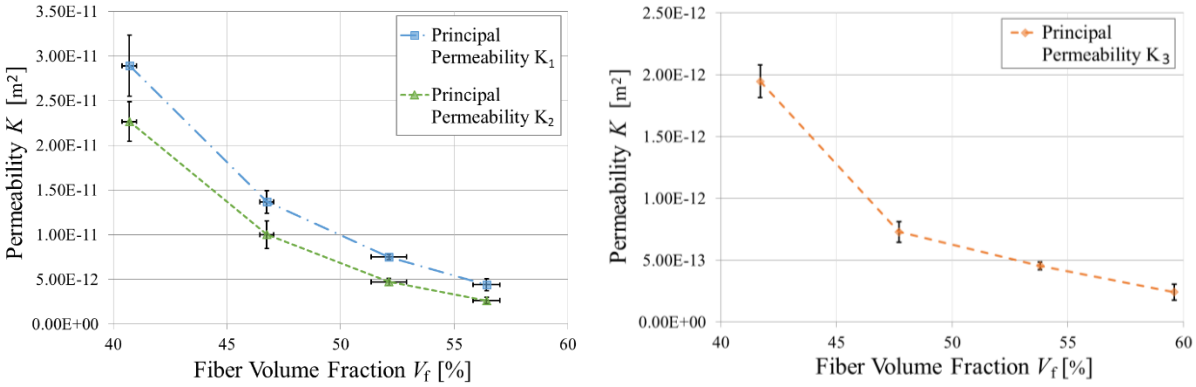

Figure 3: Principal in-plane and out-of-plane permeabilities over fiber volume fraction (mean of tests performed in triplicate; standard deviation shown as error bar).

Comparing the measured values of K_3 from Table 2 with K_1 or K_2 from Table 1, it should be noted that the out-of-plane permeability values are approximately one order of magnitude lower than their corresponding in-plane permeabilities for comparable FVF.

Table 1: In-plane permeabilities and angles of rotation for different fiber volume fractions (mean of tests performed in triplicate; relative standard deviation given for V_f , K_1 and K_2; standard deviation given for β).

V_f [%]	40.7 (±11.8%)	46.8 (±9.3%)	52.1(±4.0%)	56.4(±14.5%)
K_1 [m²]	2.89 x10^{-11} (±11.8%)	1.37 x10^{-11} (±9.3%)	7.52 x10^{-12} (±4.0%)	4.4 x10^{-12} (±14.5%)
K_2 [m²]	2.27 x10^{-11} (±9.8%)	1.0 x10^{-11} (±15.4%)	4.72 x10^{-12} (±8.4%)	2.64 x10^{-12} (±12.3%)
β	2.0° (±8.7°)	-11.4° (±8.4°)	5.6° (±6.3°)	3.7° (±2.8°)

Table 2: Out-of-plane permeabilities for different fiber volume fractions (mean of tests performed in triplicate; relative standard deviation given for K_3).

V_f [%]	41.7	47.7	53.8	59.6
K_3 [m²]	1.94 x10^{-12} (±6.7%)	7.28 x10^{-13} (±11.6%)	4.54 x10^{-13} (±6.8%)	2.41 x10^{-13} (±26.7%)

4.4. Discussion – Permeability

As CRTM simulations, based on Darcy's law, require comprehensive input data, the full permeability tensor of a carbon fiber biaxial NCF was determined over a range of process-relevant fiber volume fractions. Due to the absence of an international standard for permeability testing [19], the comparability of results between different studies is limited. An attempt to benchmark and align permeability measurements has been conducted by [17,18] and is on-going by the third benchmark series concerning radial, unsaturated in-plane permeability measurement [22]; the same method as used in the present study.

During in-plane testing, the preform height of 3 mm was controlled by the displacement control of the UTM, while additionally two laser sensors were installed to directly measure the preform thickness within the test rig. The laser sensors generally measured a larger distance than the set control value at the UTM, which can be explained by elastic deformation of the UTM and test rig during the experiments. Therefore, the corresponding FVF of each measurement was evaluated based on the laser sensors, leading to a deviation of the reported results of the in-plane measurements from the intended FVFs of the test plan.

The observed relation between permeability and fiber volume fraction correlates well with literature [9,16,23]. The reasons for some scatter in the results is seen to be the high amount of manual work during sample preparation as well as variance in the binder activation procedure for 7-layered preforms [24].

5. Compaction Behavior of Reinforcement

The reinforcement compaction behavior describes its through-thickness resistance to deformation by compression stress. Various studies describe viscoelastic compaction behavior of fibrous reinforcement material used in CFRP manufacturing. Reported viscoelastic behavior characteristics of reinforcements include strain rate dependency, stress relaxation and hysteresis [11,20].

This section presents transverse compaction tests of the carbon fiber NCF, providing stress-strain curves up to a fiber volume fraction of $V_{f,max} = 59.6\%$, which is required as input for CRTM simulation. A potential strain rate dependent compaction behavior is investigated by considering two different compaction velocities.

5.1. Experimental Procedure – Compaction

As for in-plane permeability tests, the '2D In-Plane Facility' [20] was utilized for the compaction tests. The test rig was mounted and operated on the universal testing machine (UTM) Inspekt table 100. During experiments, the compaction height h and velocity $\dot{h}$ were adjusted by the displacement control of the UTM. The compaction force was measured via a 100 kN load cell. For statistical relevance, each test set up was performed in triplicate, always using a new, untested preform.

5.2 Materials and Sample Preparation – Compaction

The same biaxial carbon fiber NCF (SIGRATEX® C B310/45-ST-E214/5g) [21] that was used for permeability characterization was also used for compaction tests. Reinforcement layers were cut into 0.3 m squares and ten layers were stacked in a manner ensuring identical biaxial fiber orientation. Preforms were binder-activated at 170°C ± 10°C via infrared heating and debulked under vacuum pressure.

5.3. Results – Compaction

Transverse compaction tests were performed at two different closing velocities: $\dot{h}_I = 1\text{mm/min}$ and $\dot{h}_{II} = 60\text{mm/min}$. Each sample was compacted to a height of 3 mm, corresponding to $V_{f,max} = 59.6\%$. The diagram in Figure 4 shows the stress-strain curves up to peak stress at maximum compaction of $V_{f,max} = 59.6\%$. For this study, strain ε is defined as:

$$\varepsilon = 1 - \frac{h}{h_0} \tag{3}$$

where h_0 represents the preform height at compaction start, recorded at a load level of 50 N. The initial preform heights of the samples for the first test series ($\dot{h}_I = 1\text{mm/min}$) were $h_{0;I} = 4.38\text{ mm} \pm 0.01\text{ mm}$, whereas a larger value of $h_{0;II} = 4.48\text{ mm} \pm 0.04\text{ mm}$ was measured for the preforms of the second test series ($\dot{h}_{II} = 60\text{mm/min}$).

Both curves in Figure 4 show a non-linear dependency between compaction stress and strain. Comparing the two curves, it should be noted that higher compaction stresses were recorded for faster compaction velocity $\dot{h}_{II}$ (for values see Table 3). For maximum compaction at $V_{f,max} = 59.6\%$ peak stresses of $\sigma_{pref;II;max} = 168.1\text{ kPa} \pm 18.2\text{ kPa}$ were measured for $\dot{h}_{II} = 60\text{ mm/min}$ and $\sigma_{pref;I;max} = 137.3\text{ kPa} \pm 4.2\text{ kPa}$ for $\dot{h}_I = 1\text{ mm/min}$.

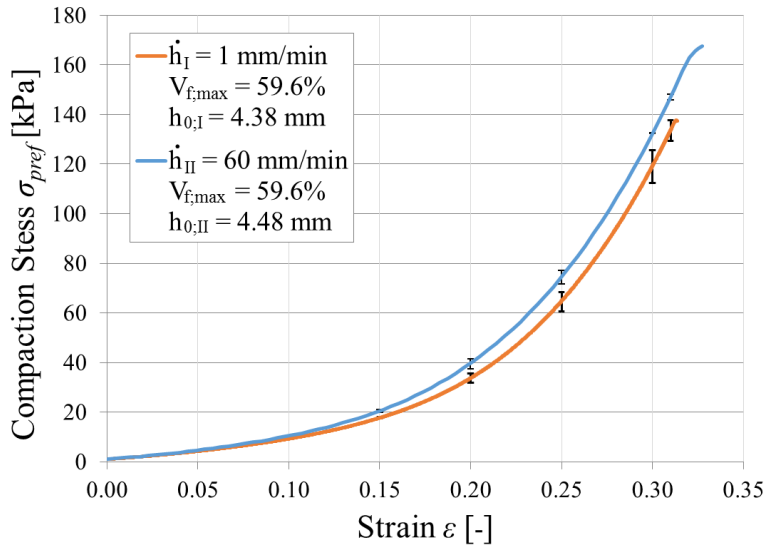

Figure 4: Stress-strain curves of compaction tests for two compaction velocities (mean of tests performed in triplicate; standard deviation shown as error bar).

Table 3: Strain ε and stress $\boldsymbol{\sigma_{pref}}$ values of compaction tests for two compaction velocities (mean of tests performed in triplicate and corresponding standard deviation).

ε [-]	0	0.05	0.1	0.15	0.2	0.25	0.3	0.31
$\sigma_{pref;I}(\dot{h}_I$=1mm/min) [kPa]	0	4.24 (±0.04)	9.26 (±0.19)	17.7 (±0.19)	33.79 (±1.82)	64.83 (±3.77)	119.33 (±6.55)	137.3 (±4.16)
$\sigma_{pref;II}(\dot{h}_{II}$=60mm/min) [kPa]	0	4.54 (±0.05)	10.51 (±0.08)	20.40 (±0.54)	38.91 (±1.97)	74.39 (±2.74)	133.71 (±0.26)	147.03 (±1.12)

5.4. Discussion – Compaction

Compaction tests of biaxial carbon fiber NCF were conducted and the material's stress-strain behavior for two different compaction velocities were presented – values which are needed as input data for CRTM simulation. The results shown in Figure 4 indicate that the compaction behavior of the material is strain-rate dependent, which agrees with the technical literature [11,20].

However, the strain, as defined in Eq. (3), depends on the initial preform height h_0 of the sample and the difference between the two initial heights $h_{0;I}$ and $h_{0;II}$ is of statistical significance. The reason for

the observed difference in initial preform heights is seen to be the low reproducibility of the binder-activation procedure. Further tests are planned to investigate the binder-activation process and its influence on compaction tests.

6. Conclusion

This paper presents input parameters required for CRTM simulation, which were determined by experimental procedures to characterize the constituent materials: resin and reinforcement. Generally, the utilized test methods are suitable for generating input data for CRTM simulations. However, the underlying assumptions of the experimental procedures need to carefully be considered when using this input data.

Viscosity measurement via rotational rheometer is a standardized procedure. Yet, it was identified that the sample preparation and dispensing process can strongly influence the transition time of the exponential viscosity rise, especially for fast curing resin systems. Furthermore, the presented input data should be expanded by characterizing the curing kinetics of the investigated resin system in order to model the complete CRTM process from preform impregnation to cured part.

All permeability tests of this study were conducted at constant preform thickness due to limited available spacers of different heights for out-of-plane tests. Therefore, the number of reinforcement layers per preform was varied to test permeabilities at different FVF levels. However, during the CRTM process, a preform with a constant number of layers is compressed, which consequently changes its permeability. The technical literature reports differences in permeability measurements of preforms containing different number of layers due to effects such as nesting or fabric pin holes [23,25]. Further investigation is required to quantify the influence that these phenomena have in the present study.

Overall, the presented material data can be employed as simulation input, providing a starting point for future CRTM software verification as well as process optimization in research and industry.

Acknowledgments

The authors would like to acknowledge KDX Europe Composites R&D Center GmbH for funding this research. The authors further thank HUNTSMAN Advanced Materials (Switzerland) GmbH for donating the investigated resin material.

References

[1] Starke J. *Carbon Composites in Automotive Structural Applications*. BMW Group. Brussels; 2016.
[2] Walbran WA, Verleye B, Bickerton S, Kelly PA. *Reducing Setup Costs: Tooling Force Prediction in Resin Transfer Moulding (RTM) and Compression RTM*. ACCE. Troy, Michigan, USA; 2009.
[3] Baskaran M, Ortiz De Mendibil I, Sarrionandia M, Aurrekoetxea J, Acosta J, Argarate U et al. *Manufacturing Cost Comparison of RTM, HP-RTM and CRTM for an Automotive Roof*. ECCM16. Seville, Spain; 2014.
[4] Advani SG, Hsiao K-T (eds.). *Manufacturing Techniques for Polymer Matrix Composites (PMCs)*. Woodhead Publishing Limited; 2012.
[5] Bickerton S, Abdullah MZ. *Modeling and Evaluation of the Filling Stage of Injection/Compression moulding*. Composites Science and Technology 2003;63(10):1359–75.
[6] Hsu S, Ehrgott M, Kelly PA. *Optimisation of Mould Filling Parameters of the Compression Resin Transfer Moulding Process*. ORSNZ Conference, Auckland, New Zealand; 2010.

[7] Le Riche R, Saouab A, Bréard J. *Coupled Compression RTM and Composite Layup Optimization. Compos. Sci. Technol*. 2003;63(15):2277–87.
[8] Verleye B, Walbran WA, Bickerton S, Kelly PA. *Simulation and Experimental Validation of Force Controlled Compression Resin Transfer Molding*. J Compos Mater 2011;45(7):815–29.
[9] Advani SG, Sozer EM. *Process Modeling in Composites Manufacturing*. New York: Marcel Dekker; 2003.
[10] Vollmer M, Baumann H, Graßl L, Schultheiß D, Mertiny P, Drechsler K. *Compression Resin Transfer Molding Simulation for Process Optimization: A User Case Study*. Luleå, Sweden; 28-29th 2018.
[11] Bickerton S, Buntain MJ, Somashekar AA. *The Viscoelastic Compression Behavior of Liquid Composite Molding Preforms*. Composites Part A: Applied Science and Manufacturing 2003;34(5):431–44.
[12] Gutowski TG, Morigaki T, Cai Z. *The Consolidation of Laminate Composites*. Journal of Composite Materials 1987;21(2):172–88.
[13] HUNTSMAN Advanced Materials. *A new Step forward in Composites Mass Production - new fast Epoxy Solution for RTM and Compression moulding*. Garching bei München; 2016.
[14] Huntsman, The Woodlands, Texas, *United States. Data Sheet: Araldite LY 3585 / Aradur 3475: Warm curing epoxy system*; 10.04.2015.
[15] Mezger T. *Das Rheologie-Handbuch: Für Anwender von Rotations- und Oszillations-Rheometern*. 4th ed. Hannover: Vincentz Network; 2012.
[16] Lomov SV. *Non-crimp Fabric Composites: Manufacturing, Properties and Applications*. Oxford, Philadelphia: Woodhead Pub; 2011.
[17] Arbter R, Beraud JM, Binetruy C, Bizet L, Bréard J, Comas-Cardona S et al. *Experimental Determination of the Permeability of Textiles: A Benchmark Exercise*. Composites Part A: Applied Science and Manufacturing 2011;42(9):1157–68.
[18] Vernet N, Ruiz E, Advani S, Alms JB, Aubert M, Barburski M et al. *Experimental Determination of the Permeability of Engineering Textiles: Benchmark II*. Composites Part A: Applied Science and Manufacturing 2014;61:172–84.
[19] Aktas A, Sims G, Lira C, Stojkovic M. *Survey of Procedures in use for Permeability Measurements in Liquid Composite Moulding Processes.* Available from: http://www.npl.co.uk/content/ConPublication/7094; 05.2016.
[20] Meier R, Walbran A, Christoph H, Zaremba S, Drechsler K. *Methods to Determine the Permeability of Textile Reinforcements*. Journal of Plastic Technology; 2014.
[21] SGL Group, Wiesbaden, Germany. *Data Sheet: SIGRATEX C B310-45/ST-E214/5g - Stitched, Biaxial, Carbon Fiber Fabric with Powder Binder*. 06.2017.
[22] David Becker. *Invitation Letter: International Benchmark on In-Plane Permeability Characterization based on Radial Flow Experiments.* 2016.
[23] Scholz S, Gillespie JW, Heider D. *Measurement of Transverse Permeability using Gaseous and Liquid Flow. Composites Part A: Applied Science and Manufacturing.* 2007;38(9):2034–40.
[24] Dickert M, Berg D, Ziegmann G. *Influence of Binder Activation and Fabric Design on the Permeability of Non-Crimp Carbon Fabrics*. FPCM11. Aukland, New Sealand; 2011.
[25] Becker D. *Transversales Imprägnierverhalten textiler Verstärkungsstrukturen für Faser-Kunststoff-Verbunde*. Dissertation. Kaiserslautern: IVW - Institut für Verbundwerkstoffe GmbH; 2015.